TEMPERATURE MAPPING OF NITROGEN-DOPED NIOBIUM SUPERCONDUCTING RADIOFREQUENCY CAVITIES*

Junki Makita[†], Old Dominion University, Norfolk, VA 23529, USA
Gianluigi Ciovati, Pashupati Dhakal, Jefferson Lab, Newport News, VA 23606, USA

Abstract

It was recently shown that diffusing nitrogen on the inner surface of superconducting radiofrequency (SRF) cavities at high temperature can improve the quality factor of the niobium cavity. However, a reduction of the quench field is also typically found. To better understand the location of rf losses and quench, we used a thermometry system to map the temperature of the outer surface of ingot Nb cavities after nitrogen doping and electropolishing. Surface temperature of the cavities was recorded while increasing the rf power and also during quenching. The results of the thermal mapping showed no precursor heating on the cavities and quenching to be ignited near the equator where the surface magnetic field is maximum. Hot-spots at the equator area during multipacting were also detected by thermal mapping.

INTRODUCTION

Over the last few years, much progress has been made on building superconducting rf resonator with high quality factor (Q_0). Achieving higher values of Q_0 could mean substantial reduction in the operational cost of an accelerator. Recent discovery to anneal Nb cavities in the presence of nitrogen or titanium have shown suppression of surface resistance up to $\sim 50\% - 70\%$ with increase of the low rf field [1, 2]. Analysis of the experimental field and temperature dependence of the surface resistance and a theory explaining the unconventional reduction of surface resistance by the rf field have been recently published [3–5]. Although the cavities doped with nitrogen or titanium have been tested to reach higher Q_0, they are limited by the quench field almost 40% lower than that of conventional undoped cavities [2].

In an attempt to understand the quench mechanism of the doped cavities, we have used an array of thermometers to map the temperatures of the outer surface of the 1.3GHz nitrogen doped single cell cavities. The thermometers are carbon resistors, whose resistance increases nearly exponentially with decreasing temperature. Fast response of the resistors and use of large number of thermometers that span the entire cavity outer surface provide powerful tool for diagnosing the quench and hot spot locations while in its operation below 4.2K. We present here the result of the temperature mappings of the nitrogen doped cavities.

EXPERIMENTAL METHOD

The thermometry system consists of 36 arrays of circuit boards each containing 16 thermometers fixed around the outer cavity surface and is based on the design developed at Cornell [6]. The boards run azimuthally around the cavity, with 10° separations, and each resistor on the board is labeled from 1 to 16, with the resistor 1 at the top iris of the cavity, 8 at the equator, and 16 at the beampipe. Temperature mapping was recorded on two single-cell ingot niobium cavities labeled TD#3 and TD#4 with resonant frequency of 1.3 GHz. After the cavities were heat treated at 800°C for 3 hours, nitrogen was injected at 25 mTorr partial pressure for 20 minutes and annealed for 30 minutes. The cavities then went through electropolishing and high-pressure rinse with ultra-pure water. On TD#3, a total of $\sim 35\,\mu m$ was removed from the inner surface by electropolishing, while on TD#4, only $\sim 10\,\mu m$ was removed. The first round of temperature mapping of the outer surface cavity was collected while ramping up the rf power up to a quench field in small increments at 2.0K and 1.6K. The temperature mapping was also recorded as rf power was ramped down from the break-down field. The cavity was then thermally cycled to above 100K, and tests were repeated.

EXPERIMENTAL RESULTS

Results of the Q_0 vs B_p measurements are summarized in Fig. 1. In both cavities, quality factors showed some improvements after the thermal cycle to above 100K. For TD#4, the cool down rate through T_c=9.25K of the cryogenic dewar was approximately 106mK/sec for the first test and 487mK/sec during the thermal cycle. For TD#3, the dewar measured the slow cooling rate of 11mK/sec for the first test and 119mK/sec during the second measurement. The vertical cryogenic dewar is cooled from the bottom, and at T_c, temperature gradients across the cavities were greater when the dewar was cooled at slower rate. During the slower cooldown, the temperature difference measured between the middle of the dewar and the bottom was $\sim 180\,K$ while the difference was $\sim 60\,K - 90\,K$ during the faster cooldown when the bottom of the dewar reached T_c. Although this result seems to be consistent with the recent work published on dependence of the residual surface resistance on the cooling dynamics, further investigation is required to fully understand the mechanism of the effect [7].

TD#3 cavity which has gone through extra amount of electropolishing compared to TD#4 showed higher break-down field, but lower quality factor. At 1.6K, TD#3 reached the breakdown field of $\sim 130 \pm 6\,mT$ while TD#4 cavity quenched at $\sim 88 \pm 4\,mT$. On the other hand, the quality
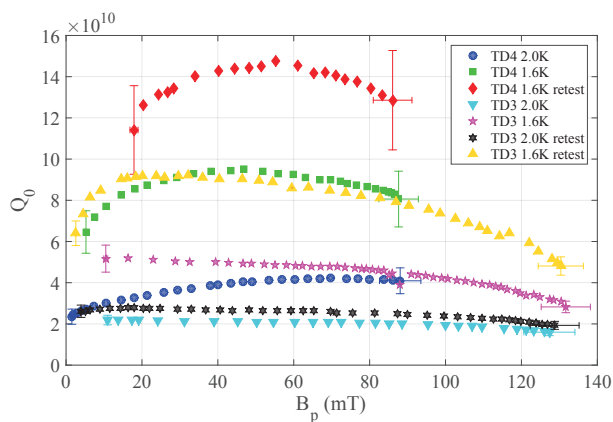
Figure 1: Q_0 vs. B_p curve for TD#3 and TD#4. 'Retest' indicates measurements after the thermal cycle.

factor at the break down field of TD#4 at 1.6K after the thermal cycle was $\sim 1.3 \times 10^{11}$ which is almost three times as large as that of TD#3 which recorded $\sim 4.8 \times 10^{10}$ at 1.6 K. While increasing the rf power on TD#3 at 1.6 K, processing of multipacting occurred at $B_p = 85$ mT, which is indicated by the small dip on the TD#3 plots on Fig. 1. We did not see the multipacting during the second measurements after the thermal cycle. The $Q(B_p)$ dependences are further analyzed in detail in Ref. [8].

The temperature maps of TD#3 before and while quenching are shown in Fig. 2. The plots show the temperature difference ΔT between helium bath and cavity outer surface. Significant heating was recorded near the equator of both cavities where the magnetic field is high. Quench was ignited at the equator, and this was detected by the temperature spike of ~ 700 mK on resistor 7, board 17 which is ~ 1 cm above the equator weld. The quench location was the same before and after the thermal cycle for both cavities. For TD#4, a couple of hot spots were located near the top iris as shown in Fig. 3. In contrast to TD#3, heating along the equator is less pronounced, and the overall heating is also suppressed. The highest ΔT during quenching was ~ 175 mK located at about 2 cm below the equator weld.

Figure 4 shows sample plots of ΔT vs. applied B_p on two locations of TD#3 before and after the thermal cycle. The plots show the temperature measured during the ramp-up and ramp-down of the rf field after reaching the breakdown field. An increase of local ΔT at locations marked with circles in Fig. 2 resulted after processing multipacting during the first measurement, as shown for example in Fig. 4 (bottom) at $B_p = 85$ mT. For TD#3, typical values of ΔT's on hot spots at the highest gradient (right before quenching) ranged from 20 mK to 150 mK at 1.6 K. After the thermal cycle, ΔT's on most of the hot spots were less than 20 mK, but this reduction in overall temperatures is most likely due to lack of multipacting. For TD#4 we did not see any multipacting, and ΔT's on hot spots at the highest gradient were less than 8 mK both before and after thermal cycle. The log-log plots of ΔT vs. B_p on hot spots showed straight
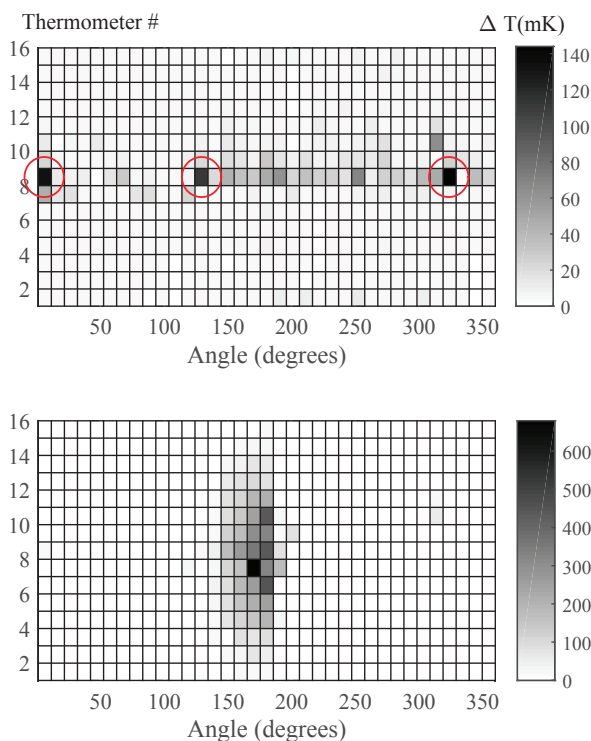

Figure 2: Temperature maps at 1.6K on TD#3 just before quench (top) and during quench at B_p=130 mT (bottom).
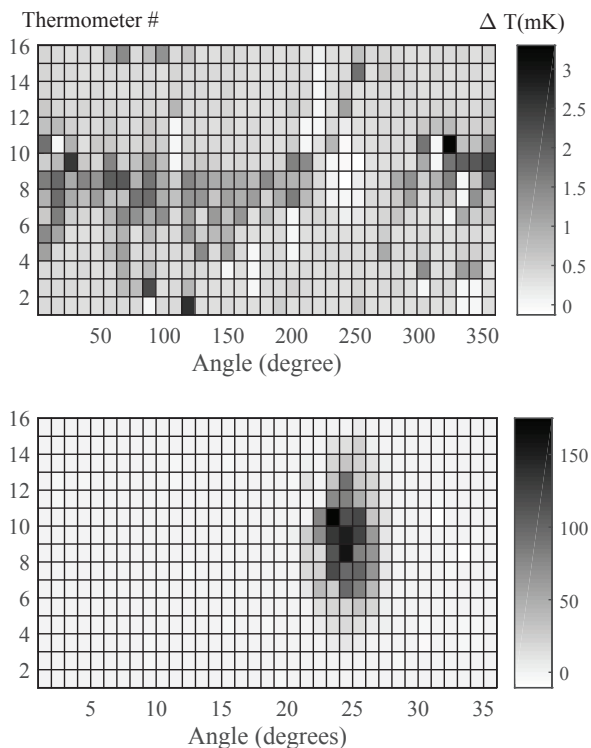

Figure 3: Temperature maps at 1.6K on TD#4 just before quench (top) and during quench at B_p=88 mT (bottom).

line with slopes ranging between 2.3 and 3.0, suggesting stronger power dissipation than simple Joule heating. Shown in Fig. 4 (top), the temperature on thermometer 8 on board 18 jumps to ~ 180 mT after quenching, and such hysteretic changes in ΔT were seen on only one or two spots on both TD#3 and TD#4 cavities. Such phenomenon is most likely attributed to trapping of Abrikosov vortices when local area of the cavity cycled between normal to superconducting state while multipacting processing and quenching [9]. Trapped flux was measured at the same location (top in Fig. 4) after quenching after the thermal cycle. $\Delta T(B_p)$ curve at quench locations at both TD#3 and TD#4 are shown in Fig. 5. The quench locations at both TD#3 and TD#4 show no significant precursor heating prior to quenching, suggesting the possibility of magnetic, rather than thermal, origin of the quench.
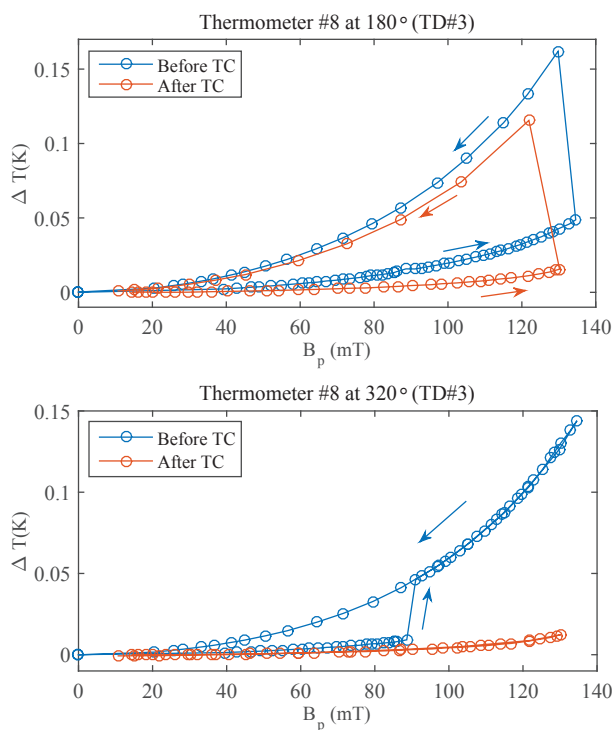

Figure 4: ΔT measured at two locations before and after thermal cycle on TD#3 at 1.6K. Top: Effect of trapped vortices on ΔT can be seen during the ramp-down of rf power. Bottom: ΔT curve is influenced by multipacting before the thermal cycle.

CONCLUSION

The temperature maps of two nitrogen-doped cavities have shown hot spots to be found near the equator. The results also revealed locations of trapped vortices resulting from multipacting processing and quenching. More heating was seen on the TD#3 cavity than on TD#4, and this is consistent with the lower quality factor measured on TD#3 after 35 µm EP. As a next step, the electronic density of states on the hot and cold spots from the cavities will be measured to
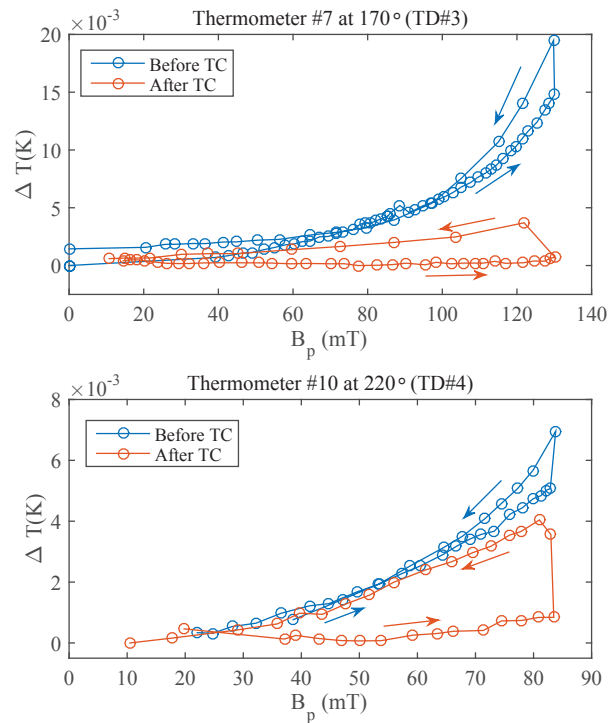

Figure 5: ΔT measured at quench locations for TD#3 (top) and TD#4 (bottom) before and after the thermal cycle.

understand the significance of nitrogen doping on enhanced quality factor and the degrading of the breakdown field.

REFERENCES

[1] P. Dhakal et al., Phys. Rev. ST Accel. Beams 16, 42001 (2013).

[2] A. Grassellino et al., Supercond. Sci. Technol. 26, 102001 (2013).

[3] G. Ciovati, P. Dhakal, and A. gurevich, Appl. Phys. Lett. 104, 092601 (2014).

[4] A. Gurevich, Phys. Rev. Lett. 113, 087001 (2014).

[5] D. Gonnella and M. Liepe, "New Insights into Heat Treatment of SRF Cavities in a Low-pressure Nitrogen Atmosphere", IPAC'14, Dresden, Germany, p.2634.

[6] J. Knobloch, H. Muller, and H. Padamsee, Rev. Sci. Instrum., 65, 3521 (1994).

[7] A. Romanenko, A. Grassellino, O. Melnychuk, and D. A. Sergatskov, J. Appl. Phys. 115, 184903 (2014).

[8] P. Dhakal, et al., "Nitrogen Doping Study in Ingot Niobium Cavities", IPAC'15, Richmond, USA (2015).

[9] J. Knobloch, H. Padamsee, "Flux Trapping in Niobium Cavities During Breakdown Events", SRF'97, p.337